

- [8]K. Shimizu, G.M.Brown, K.Kobayashi, G.E.Thompson, G.C.Wood, *Corros.Sci.* **34** (1993) 2099
- [9]K. Shimizu, G.M.Brown, K.Kobayashi, G.E.Thompson, G.C.Wood, *Corros.Sci.* **33** (1992) 1371
- [10]T.S. Sehmbi, C.Barnes, J.J.B.Ward, *Trans. IMF*, **60** (1982) 45
- [11]J.A.Treverton, M.P.Amor, A.Bosland, *Corros.Sci.* **33** (1992) 1411
- [12]G.M.Brown, K.Shimizu, K.Kobayashi, G.E.Thompson, G.C.Wood, *Corros.Sci.* **34** (1993) 1045
- [13]B.R.W. Hinton, *Metal Finishing* **89** (1991) 15
- [14]B.R.W. Hinton, *Metal Finishing* **89** (1991) 55
- [15]M.Pourbaix, Atlas of Electrochemical Equilibria in Aqueous solutions, Second English Edition, NACE, Texas, 1974

## PITTING RESISTANCE OF TUNGSTEN IMPLANTED ALUMINIUM

J.C.S. Fernandes and M.G.S. Ferreira

Department of Chemical Engineering, Instituto Superior Técnico, 1096 Lisboa Codex, PORTUGAL  
Tel. (351-1) 8417234, Fax. (351-1) 8404589, E-mail: pcjfern@alfa.ist.utl.pt

### ABSTRACT

Tungsten can be successfully implanted on aluminium forming a solid solution. SIMS, XPS and AES analysis showed that almost no tungsten was found in the passive film formed on the alloy in 0.6M NaCl solution. The beneficial effect of tungsten in the increase of the pitting potential of the alloy is due to the ennobling of the pitting process caused by the presence of metallic tungsten. This element modifies the thermodynamics and kinetics of the dissolution and facilitates hydrogen evolution inside the incipient pits, diminishing the ability of the metal to maintain the critical pH associated to stable pitting.

**Keywords:** ion implantation, aluminium, tungsten, pitting

### INTRODUCTION

Aluminium alloys are widely used in the transport industry, especially in aeronautics, because of their light weight, high strength and good resistance to uniform corrosion. However, they exhibit very poor resistance against localized attack and, in particular, to pitting in chloride-containing solutions.

It is known that the passivity of aluminium could be enhanced by using alloying elements such as Cr, Mo, Ta, Zr and W. However, improvements in the localized corrosion resistance of aluminium using conventional alloying techniques are difficult to achieve. In fact, to enhance passivation an alloying element should be retained in solid solution, without the formation of precipitates that normally act as microgalvanic cells, increasing the localized attack. Thus, the low solubility in aluminium of the transition metals (below 1% a/o) does not allow them to influence markedly the corrosion behaviour of the alloys.

In the past ten years, several authors [1-6] have investigated the metastable Al alloys obtained by nonequilibrium alloying additions of elements such as Mo, Cr, Ta, Zr and Si, using ion implantation or sputter deposition techniques that allow the amount of solute in solid solution to be increased by several orders of magnitude. From their results it seems that all the above elements lead to an improvement of the pitting resistance of the alloy, being Mo one of the most promising. Since molybdenum and tungsten have similar metallurgical and chemical behaviours, a few works devoted to supersaturated Al-W alloys have appeared recently [7-11]. These studies evidenced the beneficial effect of W on pitting corrosion resistance, but the mechanisms involved in this enhancement are not clear yet.

In the present work the role of implanted tungsten on the pitting corrosion of aluminium is studied and an explanation for the beneficial effect of tungsten is presented.

EXPERIMENTAL

Pure aluminium disks (99.999%) were mechanically polished up to 0.25 μm in alumina suspension and implanted with W, to a fluence of 4x10<sup>16</sup> W<sup>+</sup>/cm<sup>2</sup> at energies of 40 keV and 150 keV.

Tungsten concentration depth profiles were obtained by Secondary Ion Mass Spectroscopy (SIMS), Auger Electron Spectroscopy (AES) and by Rutherford Backscattering Spectrometry (RBS) with a 2 MeV Van de Graaff accelerator, as described elsewhere [9,12]. Surface analysis of the oxide films was performed by XPS.

Potentiodynamic polarization plots at a scan rate of 500 μV/s were carried out in N<sub>2</sub>-deaerated 0.6M (3.5% w/w) NaCl solutions (pH 1 and pH 7) using a Princeton Applied Research (PAR) Model 273A potentiostat.

All the potentials are referred to the saturated calomel electrode (SCE).

RESULTS AND DISCUSSION

• Composition and structure of the implanted alloys

A typical depth profile obtained by AES for the as-implanted samples (4x10<sup>16</sup> W<sup>+</sup>/cm<sup>2</sup>, 150 keV) is presented in Fig. 1, showing a maximum of tungsten concentration (9 at%) for a depth of approximately 70 nm. The thickness of the oxide layer was determined as the depth at which the oxygen signal has dropped to half of its maximum value, leading to a value of 20 Å. Thus, the W-rich zone is located deep in the substrate metal and no tungsten is found at the metal/film interface or in the passive film.

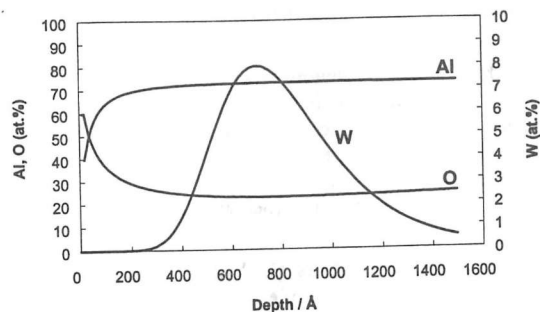


Figure 1 - Depth profile obtained by AES for as-implanted samples (4x10<sup>16</sup> W<sup>+</sup>, 150 keV)

The W depth profiles obtained by AES for the two different implantation energies (40 keV and 150 keV) are compared in Fig.2. As expected, for the same fluence, higher energies lead to a broader W-rich zone with a lower maximum concentration of tungsten and located deeper in the substrate metal.

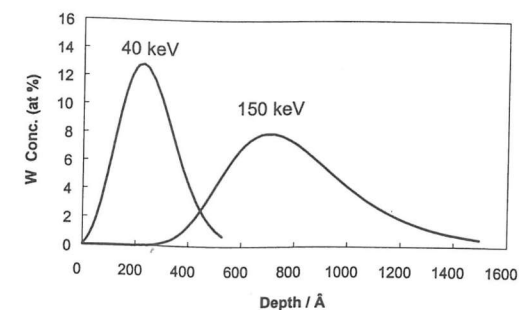


Figure 2 - Depth profiles obtained by AES for samples implanted at different energies (4x10<sup>16</sup> W<sup>+</sup>, 40 keV and 150 keV)

XPS measurements were performed with implanted samples in three different conditions: as received, after 1h immersion in 0.6M NaCl solution and after anodic polarization up to the pitting potential in the same solution. In all cases no tungsten was found in the surface passive film, meaning that, if there is some W, its concentration should lie below the detection limit of the instrument (usually 0.3%).

SIMS profiles obtained on samples implanted at an energy of 40 keV suggest that W is present in the surface, although in small amount (Fig. 3).

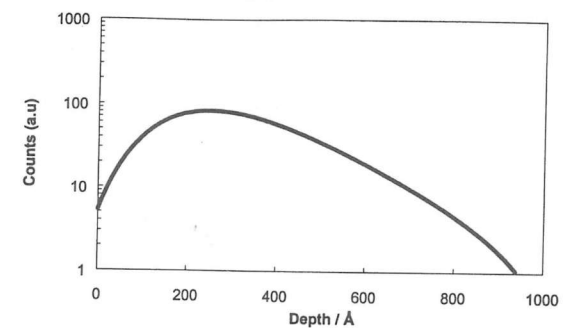


Figure 3 - Depth profile obtained by SIMS for as-implanted samples (4x10<sup>16</sup> W<sup>+</sup>, 40 keV)

Rutherford Backscattering Spectrometry (RBS) was used to compare the W depth profiles for the implanted alloys in the same three different conditions. When plotting the results (Fig.4), the zero of the depth scale was set at the metal/film interface. Comparing the profiles for the three conditions (Fig. 4) no difference is found, which means that, from a macroscopic point-of-view, the W-rich implanted layer was not affected and, in particular, no W enrichment at the metal/film interface occurred. In fact, the pits generated during anodic polarization should lead to a different response but, due to the limited lateral resolution of RBS, these microscopic heterogeneities are not detected.

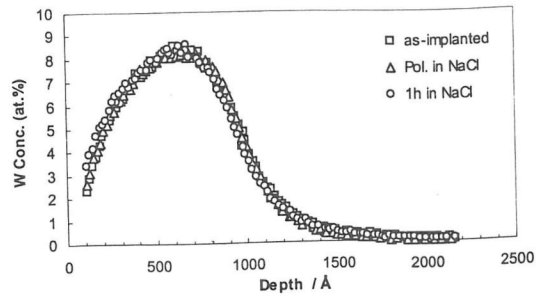


Figure 4 - Tungsten depth profiles (RBS) for implanted alloys: as-received, after 1h immersion in 0.6M NaCl and after anodic polarization up to the pitting potential in 0.6M NaCl

Grazing Incidence X-Ray Diffraction (GIXRD) was used to determine the metallurgical stability of the implanted alloys shortly after implantation and after several months. An Al-type structure was found, with the (111), (200), (220) and (311) planes diffracting the beam (Fig.5). All the Al diffraction peaks were shifted to higher angles, indicating that smaller W atoms had substitutionally replaced Al in the substrate face-centered-cubic lattice, decreasing the lattice parameter. No evidence of intermetallic phase formation was found, even 10 months after implantation. The formation of precipitates would increase the corrosion and pitting susceptibility of the alloys.

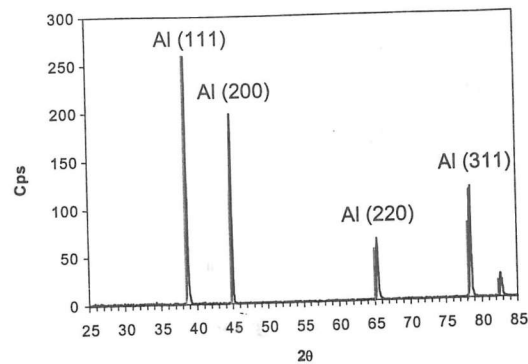


Figure 5 - GIXRD patterns for as-implanted samples (pure Al standard diffraction peaks are represented by dashed lines)

• Polarization plots

Figure 6 shows the anodic polarization plots for pure aluminium and W implanted aluminium. Apart the differences in the free corrosion potential already mentioned, the passive current and the pitting potential are respectively lower and higher for the implanted specimens.

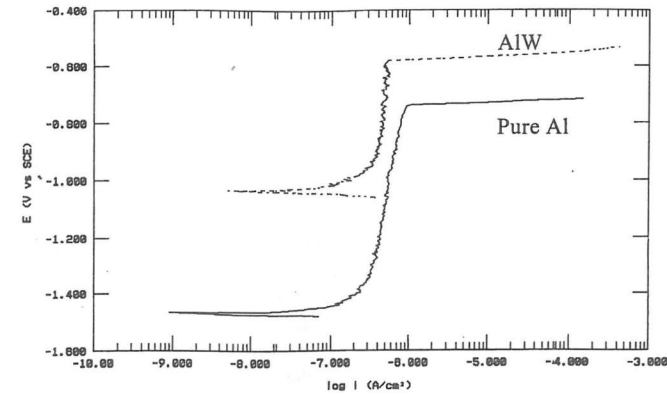


Figure 6 - Anodic polarization plots for pure Al and W implanted aluminium in 0.6 M NaCl solutions (pH7)

Frankel, Newman et al [13] analysed the pitting resistance of sputter-deposited aluminium alloys and put forward the idea that stable pitting initiation is related to both pit growth and passive film effects. Since stable pit growth is not possible below the repassivation potential, the portion of the increase in pitting potential for an alloy, from that of pure aluminium to the repassivation potential of the alloy, results from pit growth factors. Moreover, as stable pits do not initiate until the pitting potential is reached, because of the protection provided by the passive film, the difference between the repassivation potential of the alloy and its pitting potential is the added effect of the protection provided by the alloy passive film [13]. The relative weight of the two factors depends on the solute element, the latter effect being determinant in the case of elements that form promptly good protective films.

In the present case, the analysis results show that there is almost no W in the passive film. AES and XPS were unable to detect it and only SIMS indicates its presence. Thus the role of W on pitting initiation of aluminium should be mainly related to its effect on pit growth factors rather than the properties of tungsten oxide.

Pit growth considerations are mainly related to the ability of the metal to maintain a critical pH inside the incipient pits, which depends on the critical concentration of metal ions in the pit electrolyte that, by hydrolysis, generate H<sup>+</sup> ions, and on the consumption of these H<sup>+</sup> ions. In the present case the factors affecting these phenomena should be related to the ennobling of the dissolution process of the alloy and the current efficiency in the pits. The ennobling of the dissolution process is controlled by both thermodynamics, through the reversible potential of the alloy in the pit environment, and kinetics, through the exchange current density. On the other hand, the current efficiency is controlled by hydrogen evolution inside the pits which increases the local pH (Fig.7).

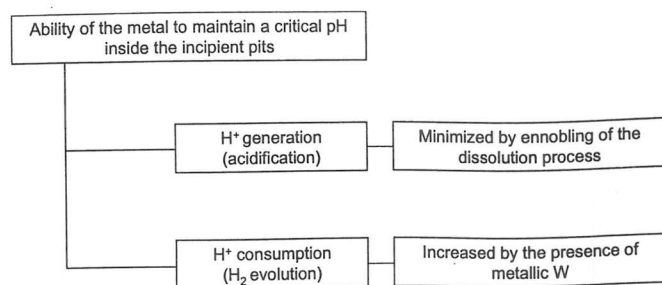


Figure 7 - Factors that affect the attainment of the critical pH inside the incipient pits

The reversible potential of tungsten is far greater than aluminium, which makes at least the thermodynamics of the alloy less favourable to dissolution. Assuming uniform dissolution of the alloy, its corrosion rate is dependent on the corrosion rates of the constituents and on the mole fractions they are present in the alloy. Owing to faster dissolution of the more reactive component, i.e. Al, the alloy surface becomes enriched in W so that the mole fraction of this element increases in the alloy, slowing down its rate of dissolution. Moreover the exchange current density for the hydrogen evolution reaction can be five orders of magnitude larger on W than on Al [14] which leads to a much higher rate of hydrogen evolution in the case of the W implanted alloy. This fact makes more difficult the attainment of the critical pH inside the pits, then contributing for retarding the establishment of stable pits.

#### REFERENCES

- [1] A. H. Al-Saffar, V. Ashworth, A. K. O. Bairamov, D. J. Chivers, W. A. Grant and R. P. M. Procter, *Corros. Sci.*, **20** (1980), 127
- [2] P. M. Natishan, E. McCafferty and G. K. Hubler, *J. Electrochem. Soc.*, **133** (1986), 1061
- [3] W. C. Moshier, G. D. Davis, J. S. Ahearn and H. F. Hough, *J. Electrochem. Soc.*, **133** (1986), 1063
- [4] W. C. Moshier, G. D. Davis, J. S. Ahearn and H. F. Hough, *J. Electrochem. Soc.*, **134** (1987), 2677
- [5] P. M. Natishan, E. McCafferty and G. K. Hubler, *J. Electrochem. Soc.*, **135** (1988), 321
- [6] G. D. Davis, W. C. Moshier, T. L. Fritz and G. O. Cote, *J. Electrochem. Soc.*, **137** (1990), 422
- [7] B. A. Shaw, T. L. Fritz, G. D. Davis and W. C. Moshier, *J. Electrochem. Soc.*, **137** (1990), 1317
- [8] B. A. Shaw, G. D. Davis, T. L. Fritz, B. J. Rees and W. C. Moshier, *J. Electrochem. Soc.*, **138** (1991), 3288
- [9] R. C. Da Silva, M. F. Da Silva, A. A. Melo, J. C. Soares, E. Leitão and M. Barbosa, *Nuclear Instruments and Methods in Physics Research*, **B50** (1990), 423
- [10] J. C. S. Fernandes and M. G. S. Ferreira, *Surface and Coatings Tech.*, **56** (1992), 75
- [11] G.D. Davis, B.A. Shaw, B.J. Rees and M. Ferry, *J. Electrochem. Soc.*, **140** (1993), 951
- [12] M. F. Da Silva, M. R. Da Silva, E. Alves, A. Melo, J. C. Soares, J. Winand and R. Vianden, in *Surface Engineering*, eds. R. Kossowsky and S. C. Singhal, NATO ASI Series E85, Martinus Nijhoff (1984), p.74
- [13] G.S. Frankel, R.C. Newman, C.V. Jahnes and M.A. Russak, *J. Electrochem. Soc.*, **140** (1993), 2192
- [14] J.M. West, "Electrodeposition and Corrosion Processes", Van Nostrand Reinhold Company, London (1970)

## APPLICATION OF CYCLIC VOLTAMMETRIC TECHNIQUE ON DYE CONCENTRATION CONTROL IN AQUEOUS SOLUTIONS

M. de Fátima Esteves<sup>1\*</sup>, M.T.Pessoa de Amorim<sup>1</sup>, C. Comel<sup>2</sup>

<sup>1</sup>*Departamento de Engenharia Têxtil, Escola de Engenharia, Universidade do Minho, P-4800 Guimarães*

<sup>2</sup>*Laboratoire de Chimie et Environnement, U.F.R. Sciences, Université d'Angers, F-49045 Angers Cedex*

#### Abstract

This communication follows a previous work concerning indirect electrochemical reduction of dyes [1] and its application on dyeing control with sulphur dyes.

The study concerns the cathodic peak intensity variation with sulphur dye C.I. Leuco Sulphur Black 1 (Black Diresul RDT liq.) concentration, in the presence of a mediator, iron/triethanolamine (Fe<sup>III</sup>/TEA), in alkaline media.

**Key Words:** Mediator redox couple, reversible electron-transfer, cathodic peak intensity, dye concentration

#### 1. Introduction

Earlier cyclic voltammetric studies with glass carbon electrodes [1] showed a linear correlation between cathodic peak intensity and dye concentration. Experimental